The *n*-Alcohol Site in the Nicotinic Receptor Pore Is a Hydrophobic Patch†

Qiong L. Zhou,‡,§ Qing Zhou,‡,§ and Stuart A. Forman*,‡,||

Department of Anesthesia and Critical Care, Massachusetts General Hospital, and Department of Anaesthesia, Harvard Medical School, Boston, Massachusetts 02114

Received June 5, 2000; Revised Manuscript Received September 12, 2000

ABSTRACT: Alcohols and volatile anesthetics inhibit peripheral nicotinic acetylcholine receptors noncompetitively, primarily via an open-channel block mechanism. Analysis of hydrophobic mutations near the middle of the pore-forming M2 domains suggested that alcohols interact with the pore in this vicinity. To establish the extent of this inhibitory site, we created a series of hydrophobicity-altering mutations scanning most of the α subunit M2 domain. Using both single-channel and rapid patch perfusion electrophysiology, we measured how these mutations affect nAChR sensitivity to ethanol and hexanol. We find a near-contiguous series of amino acids in α-M2, extending from αL250 (8′) to αV255 (13′), where mutagenesis strongly influences inhibition by alcohols. These results support the existence of a large inhibitory patch in the nAChR pore lining where interactions with alcohols are primarily due to hydrophobic forces. Ethanol appears to interact with deeper regions of this site than does hexanol. Because alcohols apparently act as open-channel blockers, we infer from our results that most of the residues between αL250 and αV255 are exposed to the aqueous environment of the pore when the channel is open. The location and extent of this site can explain why small alcohols occupy the nAChR pore at the same time as larger alcohols or charged blockers, while two large alcohols bind in a mutually exclusive manner.

Ligand-gated ion channels (LGICs) are important regulators of neuronal excitability and likely molecular targets where anesthetics and alcohols act in the central nervous system (*1*, *2*). Peripheral nicotinic acetylcholine receptors (nAChRs),[1] like LGICs found in the CNS, are sensitive to anesthetics and alcohols. Furthermore, the structure and dynamic behavior of peripheral nAChRs are far better defined than those of related CNS channels, in large part because of the ability to isolate milligram quantities of purified nAChR protein from *Torpedo* electroplaque. *Torpedo* nAChRs and their close relatives from mammalian neuromuscular junctions consist of five homologous subunits, two α, one *β*, one *γ*, and one *δ*, which are arranged symmetrically around the central cation-conducting transmembrane pore (*3*). Each subunit contains a large amino-terminal extracellular domain and four hydrophobic transmembrane domains (M1−M4). The agonist sites, which bind ACh as well as competitive antagonists, are formed by the extracellular domains at the α−*γ* and α−*δ* subunit interfaces. The transmembrane pore is formed by amino acids from the five M2 domains, each of which is supposed to form an α-helical structure traversing the lipid bilayer. Most of the M2 domain residues on nAChR subunits are hydrophobic, with some hydrophilic residues, in roughly homologous locations (4′, 6′, 10′, and 12′; see Table 1).

It has been hypothesized that sensitive LGICs possess anesthetic binding sites. We have identified a functional anesthetic/alcohol site within the transmembrane pore of peripheral nAChRs from both *Torpedo* electroplaque and mammalian neuromuscular junction. Evidence for this site came first from kinetic studies, where it was observed that potent anesthetic alcohols such as octanol inhibit nAChR function mostly by acting after the channel opens in the presence of agonists (*4*). Single-channel kinetic analyses of nAChR currents in the presence of a variety of general anesthetic compounds also support the idea that a large fraction of inhibition is due to open-channel blockade (*5*, *6*). Another critical piece of evidence was the finding that in *Torpedo* nAChR inhibition assays, two potent alcohol inhibitors act in a mutually exclusive manner, indicating that they compete for a single shared site of action (*7*). More recently, a photoactivatable long-chain alcohol was synthesized and shown to photolabel the M2 domain of *Torpedo* nAChR α subunits (*8*, *9*). Mutation of an amino acid located near the middle of the murine nAChR α-M2 domain (αS252 or αS10′) from serine to different hydrophobic side chains dramatically increases the sensitivity of nAChRs to inhibition (assessed electrophysiologically) by alcohol and volatile anesthetics (*10*). Importantly, the sensitivity to anesthetic inhibition correlates strongly with the hydrophobicity of the mutated side chain, consistent with the long-established tenet that anesthetic potency is highly dependent on hydrophobic interactions. Investigation of homologous mutations at the 10′ positions of M2 domains on *β*, *γ*, and *δ* nAChR subunits showed that all five M2 domains independently and simul-

† This research was supported by grants from the NIH (K21AA00206 and P01GM58448) to S.A.F.

* To whom correspondence should be addressed: Department of Anesthesia and Critical Care, CLN-3, Massachusetts General Hospital, Boston, MA 02114. Phone: (617) 724-5156. Fax: (617) 724-2712. E-mail: forman@helix.mgh.harvard.edu.

‡ Department of Anesthesia and Critical Care, Massachusetts General Hospital.

§ These authors contributed equally to this research.

|| Department of Anaesthesia, Harvard Medical School.

[1] Abbreviations: ACh, acetylcholine; EtOH, ethanol; nAChR, nicotinic acetylcholine receptor.

10.1021/bi001281q CCC: $19.00
Published on Web 11/02/2000

Table 1: Amino Acid Sequences of Mouse Muscle M2 Domains[a]

		1′	2′	3′	4′	5′	6′	7′	8′	9′	10′	11′	12′	13′	14′	15′	16′	17′	18′	19′	20′
α	K242	M	T	L	S	I	S	V	L	L	S	L	T	V	F	L	L	V	I	V	E
β	K253	M	G	L	S	I	F	A	L	L	T	L	T	V	F	L	L	L	L	A	D
γ	K251	C	T	V	A	T	N	V	L	L	A	Q	T	V	F	L	F	L	V	A	K
δ	K256	T	S	V	A	I	S	V	L	L	A	Q	S	V	F	L	L	L	I	S	K

[a] Sequence alignment and terminology following that of Miller (*31*). The first residue is numbered from the amino terminus, which is supposed to be at the cytoplasmic end of the pore. Single-letter amino acid code: A, alanine; C, cysteine; D, aspartate; E, glutamate; F, phenylalanine; G, glycine; H, histidine; I, isoleucine; K, lysine; L, leucine; M, methionine; N, asparagine; P, proline; Q, glutamine; R, arginine; S, serine; T, threonine; V, valine; W, tryptophan; Y, tyrosine.

taneously interact with alcohol inhibitors, indicating that the site is within the central pore rather than at a number of independent sites on separate subunits (*11*).

While the combined results of these kinetic, pharmacological, photolabeling, and mutational/functional experiments leave little doubt that an anesthetic/alcohol binding site exists near the middle of the nAChR pore, the overall extent of this site remains unexplored. Indeed, we have suggested that the hydrophilic side chain of αS10′ is unlikely to be involved in hydrophobic interactions and that nearby leucines at positions 8′ and 9′ are more likely to form a hydrophobic site where anesthetics bind (*10*). Others have noted that blockers with differing sizes or from different molecular classes apparently do not compete for occupation of nAChR inhibition sites (*12*, *13*). Thus, different compounds may interact with different portions of the nAChR pore. One model that has been proposed to accommodate these results is one in which the nAChR site contains a large "hydrophobic patch" where interactions by multiple compounds can inhibit function, without necessarily interfering with binding by other compounds (*12*).

To probe the extent of the nAChR pore site, we applied the hydrophobic mutagenesis[2] approach to other α-M2 residues, scanning from αS4′ (near the cytoplasmic end of M2) to αL16′ (near the extracellular end of M2). At each position, we made a mutation that considerably alters the hydrophobicity of the wild-type amino acid. We evaluated the sensitivity of these mutant nAChRs to hexanol, a potent anesthetic alcohol, as well as ethanol, a much smaller alcohol that weakly interacts with the pore site (*14*, *15*).

MATERIALS AND METHODS

Site-Directed Mutagenesis. cDNAs for the α, *β*, *γ*, and *δ* subunits of the mouse muscle nAChR were subcloned into pSP64T plasmids containing *Xenopus* globin noncoding sequences (generously supplied by J. McLaughlin, Medical University of South Carolina, Charleston, SC). Mutations were introduced into the mouse α subunit cDNA using oligonucleotide-directed mutagenesis on the wild-type template (*11*). The αL9′T cDNA was provided by M. M. White (Allegheny University, Philadelphia, PA) and transferred into the pSP64T vector. All mutations and transferred sequences were confirmed by dideoxynucleotide sequencing.

Xenopus Oocyte Expression. Methods for oocyte expression were previously described (*10*). After incubation for 48−72 h, oocytes were stripped of their vitelline membranes so patch-clamp electrophysiology could be carried out.

[2] We use the terms "hydrophobic mutation" and "hydrophobic mutagenesis" to reflect our strategy of mutations that cause large increases and decreases in side chain hydrophobicity, respectively.

Patch-Clamp Electrophysiology. Multichannel rapid patch superfusion and single-channel experiments were performed at room temperature (20−22 °C). Patch pipets were fire-polished to give an open tip resistance of 2−4 MΩ. For rapid superfusion studies, oocyte membrane patches were excised in the outside-out configuration and held at −50 mV. For single-channel recordings, oocyte patches were sealed in the on-cell or excised inside-out configuration. Inside and outside buffers were symmetrical K-100 buffers (97 mM KCl, 1 mM $MgCl_2$, 0.2 mM EGTA, and 5 mM K-Hepes, pH adjusted to 7.5 with KOH). Currents through the patch-clamp amplifier (Axopatch 200A or 200B; Axon Instruments, Foster City, CA) were filtered (eight-pole bessel, 2−5 kHz) and digitized at 5−10 kHz.

Rapid Patch Superfusion. Rapid superfusate switching (0.2−1.2 ms, measured with open pipet junction currents) was achieved using piezo-driven theta tube or quad tube devices that have been described previously (*11*, *16*). ACh exposure periods were between 50 and 10 000 ms, and patches were recovered in control superfusate for 5−20 s between ACh exposures.

Measurement of ACh EC_{50}s and Desensitization Time Constants. ACh EC_{50}s and the Hill slopes (n_H) of gating for all nAChRs were determined using rapid superfusion electrophysiology. Peak currents were measured over a range of ACh concentrations and normalized to control peak currents at high ACh concentrations (1 mM) recorded in the same patch. Patch current rundown was minimized by utilizing the quad-superfusion device, which enabled rapid alteration between control and experimental stimulations. For each receptor type, normalized data from at least three patches were pooled. Logistic functions of the form $I/I_{cntl} = [ACh]^{n_H}/([ACh]^{n_H} + EC_{50}^{n_H})$ were fitted to normalized data by nonlinear least-squares methods. Desensitization time constants were determined from rapid superfusion recordings at maximal ACh concentrations ($\geq 10 \times EC_{50}$). Currents from a minimum of three separate patches were recorded during ACh pulses of up to 10 s, and rapid desensitization time constants were derived from single-exponential fits to the declining phases of the currents during ACh exposure. Addition of a second exponential component to fits did not significantly improve the quality of the fits (*F* test).

Inhibition of Multichannel Patch Currents by Hexanol. Hexanol (>99.5% pure) was purchased from Fluka Chemical Co. and weighed directly into K-100 to make stock solutions, which were stored in glass and diluted immediately prior to use in experiments. Solution flowed continuously from glass reservoirs to the superfusion pipets through PTFE and glass tubing.

Rapid multichannel current traces displayed in the figures are ensemble averages of 4−16 sequential recordings from

Table 2: Effects of nAChR α-M2 Hydrophobic Mutations on Channel Conductance, Gating, and Desensitization

nAChR type	$\Delta H\Phi$[a]	Δarea[b] (Å^2)	γ_{0-EtOH} (pS)	ACh EC_{50} (μM)	n_H	τ_{des} (ms)	alcohol sensitivity[c]
wild type	0	0	54 ± 2.2	18 ± 2.1	2.0 ± 0.23	140 ± 55	
αS4′L	4.6	55	50 ± 1.5	14 ± 3.6	1.5 ± 0.37	180 ± 48	NS/NS
αI5′S	−5.3	−55	44 ± 2.2	21 ± 1.7	2.1 ± 0.30	280 ± 52	NS/NS
αS6′F	3.6	95	42 ± 2.0	3.6 ± 0.39	1.6 ± 0.21	130 ± 47	NS/NS
αV7′A	−2.4	−40	43 ± 2.8	6.6 ± 0.22	1.8 ± 0.10	320 ± 140	NS/NS
αL8′S	−4.6	−55	42 ± 1.3	110 ± 19	1.5 ± 0.32	130 ± 26	NS/− −
αL9′T	−4.5	−30	62 ± 1.6	0.20 ± 0.016	1.5 ± 0.13	>10000	− −/− −
αS10′I	5.3	60	45 ± 3.3	11 ± 1.0	1.8 ± 0.12	50 ± 27	++/++
αL11′S	−4.6	−55	47 ± 0.7	1.0 ± 0.12	2.1 ± 0.45	140 ± 25	−/− −
αT12′I	5.2	35	35 ± 0.5	1.7 ± 0.16	1.9 ± 0.27	>10000	−/NS
αV13′S	−5.0	−40	52 ± 4.5	0.20 ± 0.031	1.5 ± 0.19	>10000	− −/− −
αF14′S	−3.6	−95	44 ± 1.8	2.4 ± 0.57	1.6 ± 0.27	190 ± 89	NS/NS
αL15′S	−4.6	−55	51 ± 2.3	8.2 ± 0.39	1.7 ± 0.14	220 ± 56	NS/NS
αL16′S	−4.6	−55	48 ± 2.5	1.0 ± 0.25	1.6 ± 0.14	>10000	NS/NS

[a] Hydrophobicity is in arbitrary units from the scale by Kyte and Doolittle (*17*). [b] Area is the accessible surface area as reported by Chothia (*18*). [c] The degree of increase (+) or decrease (−) in sensitivity to nAChR inhibition by hexanol or ethanol associated with each mutation is indicated. NS indicates no significant change.

a single patch. Control currents (saturating ACh concentration alone, usually 1 mM) were recorded both before and after experiments where patches were exposed to 0.5 mM hexanol. When a theta tube was used for rapid superfusion, hexanol was added to both superfusate solutions (buffer and ACh). When quad tubes were used, patches remained in alcohol-free buffer and were exposed to hexanol solution for ≥0.2 s prior to exposure to the hexanol/ACh solution. Data were not analyzed if the pre- and postcontrol peak currents differed by more than 10%. To calculate the percent inhibition by hexanol, peak currents were first baseline corrected and the peak current in hexanol was normalized to the average of the pre- and postcontrol peaks.

Reduction of Single-Channel Conductance by Ethanol. Single-channel conductances were measured in the presence of low ACh concentrations (0.02−2 μM) and the same or a lower ACh concentration with ethanol. For these experiments, patches were voltage-clamped in the on-cell or inside-out configuration with ACh inside the pipet. Current traces were recorded (5−10 kHz sampling with a 2 kHz bessel filter) during 6 s voltage ramps from 150 to −50 mV. Conductance was calculated as the difference in the slopes (*pA*/*V*) between the baseline and single openings (*15*).

Statistical Analysis of Mutant Effects. Values are reported as means ± the standard deviation. Linear and nonlinear least-squares analyses and Student's *t* tests were performed using commercial software (Origin, Microcal Inc., Northampton, MA). Multichannel hexanol inhibition data for mutant nAChRs were compared pairwise to wild-type results using two-tailed Student's *t* tests. To compare the inhibitory effects of EtOH in mutants with those in wild-type nAChRs, we pooled unpaired apparent conductance measurements and calculated percent inhibition. Standard deviations for these values were calculated by the delta method. *p* values (two-tailed) for pairwise comparisons between mutants and the wild type were derived from *z*-statistics using Instat2 software (GraphPad Software, San Diego, CA).

RESULTS

Characterization of nAChR Mutants. Our strategy in constructing mutations was to create a large change in hydrophobicity at each α-M2 domain locus that was examined, because hydrophobicity has been shown to be an important determinant of alcohol potency in both nAChRs and animal behavior tests. Since most of the wild-type amino acids in the α-M2 contain hydrophobic side chains (see Table 1), these residues were mutated to hydrophilic but uncharged amino acids such as serine (S) and threonine (T), or, in one case, alanine (A). Conversely, those wild-type amino acids that contain hydrophilic side chains were mutated to very hydrophobic amino acids such as leucine (L), isoleucine (I), or phenylalanine (F). The 13 mutations are listed in Table 2 along with the mutation-induced changes in side chain hydrophobicity and size. With one exception, the magnitudes of the changes in side chain hydrophobicity associated with the mutations were quite similar, an increase or decrease of 3.6−5.3 units on the scale developed by Kyte and Doolittle (*17*). Similarly, the changes in side chain area associated with most of these mutations fell within a narrow range, increasing or decreasing 30−60 Å^2 (*18*).

ACh-gated dynamic functions of nAChRs containing the α-M2 mutations were characterized in detail using both single-channel and rapid patch superfusion electrophysiology (Table 2). Single-channel conductances in the majority of the mutant receptors were lower than that of the wild type, and most were within 20% of the wild-type conductance (52 ± 2.2 pS). The lowest value was found for the αT12′I mutant (35 ± 0.5 pS), 67% of the wild-type value. One mutant, αL9′T, exhibited conductance that was significantly higher than that of wild-type nAChR.

ACh-dependent gating was further characterized by determining the ACh EC_{50} and Hill coefficient (n_H) in rapid patch superfusion experiments (Table 2). Five mutant receptors exhibited EC_{50} values that differed from the wild-type EC_{50} (18 ± 2.1 μM) by a factor of less than 2. Four mutant receptors (αL9′T, αL11′S, αV13′S, and αL16′S) were characterized by EC_{50}s of ≤1.0 μM. Only one mutant receptor, αL8′S, had an EC_{50} that was significantly higher than that of the wild type. All of the gating Hill coefficients were between 1.5 and 2.1.

The desensitization time constants (τ_{des}) for most α-M2 mutant nAChRs differed from the wild-type value (140 ± 55 ms) by less than a factor of 2. Four mutations (αL9′T, αT12′I, αV13′S, and αL16′S) were characterized by τ_{des} values that were greater than 10 s.

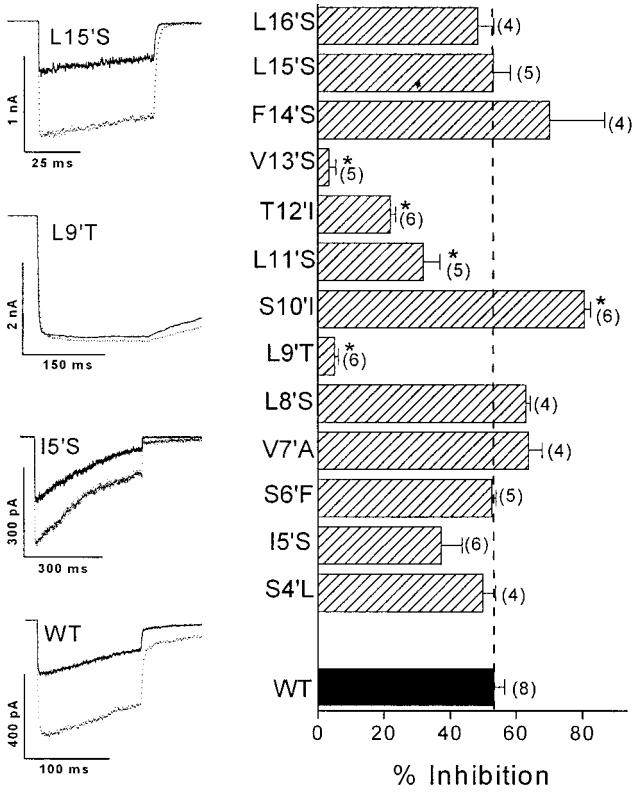

FIGURE 1: Hexanol inhibition of nAChRs containing α-M2 hydrophobic mutations. (Left) Typical traces recorded from four patches expressing wild-type nAChRs or nAChRs containing α-I5′S, α-L9′T, and α-L15′S mutations. Each panel shows a control current (···) elicited with rapidly superfused ACh (at least 10 × EC_{50}) and a paired trace recorded in 0.5 mM hexanol (—). (Right) Summary bar graph depicting the average (± the standard deviation) peak current inhibition in the presence of 0.5 mM hexanol. The number of patches studied for each receptor type is reported to the right of the bars in parentheses. The dashed vertical line represents the wild-type inhibition value. Asterisks denote inhibition values that differ from the wild type ($p \leq 0.05$).

Hexanol Inhibition. Sensitivity to inhibition by hexanol was measured using rapid patch superfusion with saturating ACh concentrations (≥10 × EC_{50}) to minimize possible effects of altered channel gating. The rapid patch superfusion technique also enabled assessment of peak ACh-induced currents on a time scale (<5 ms), during which ACh-induced desensitization was minimal (Figure 1, left panels).

As we have previously reported, peak currents elicited from patches expressing wild-type nAChRs are inhibited about half (53 ± 3.2%; $n = 8$) by 0.5 mM hexanol. We have also reported that the αS10′I mutation significantly increases nAChR sensitivity to inhibition by hexanol. When scanning toward the inner end of α-M2 is carried out, the αL9′T mutation obliterated hexanol inhibition, but hydrophobic mutations at positions 8′−4′ caused no significant change in hexanol sensitivity. When scanning toward the outer end of α-M2 was carried out, mutations αL11′S, T12′I, and V13′S all significantly reduced the sensitivity to hexanol inhibition, while mutations at positions 14′−16′ caused no significant effects. Thus, hexanol sensitivity is affected by hydrophobic mutations at a contiguous series of five α-M2 residues from positions 9′ to 13′, but unaffected by mutations at other loci that were studied (Figure 1, right panel).

Ethanol Inhibition. Because ethanol is known to both enhance nAChR gating (*19*) and reduce nAChR conductance

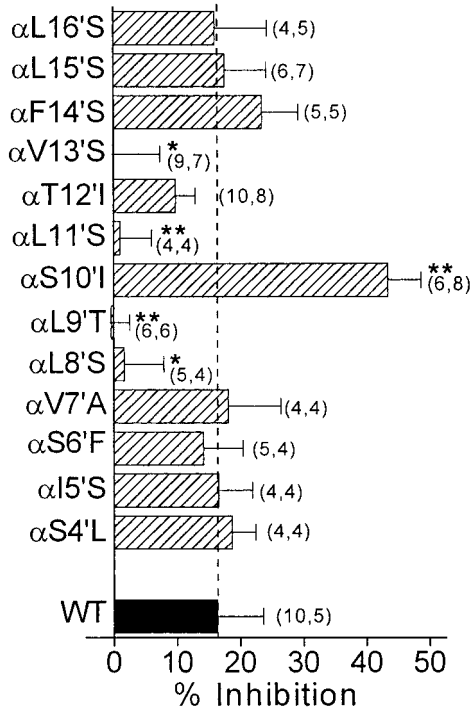

FIGURE 2: Ethanol inhibition of nAChRs containing α-M2 hydrophobic mutations. Each bar depicts the average (± the standard deviation) single-channel current reduction in the presence of 400 mM ethanol. The numbers of independent conduction determinations for each receptor type under control conditions and in the presence of ethanol are shown to the right of the bars in parentheses. The dashed vertical line represents the wild-type inhibition value. Two asterisks denote inhibition values that differ from the wild-type value ($p \leq 0.05$), and one asterisk denotes those that differ from the wild-type value ($p \leq 0.15$).

(*14*, *15*), ethanol effects on multichannel currents may reflect two independent actions, particularly if mutations decrease the likelihood of channel opening. We therefore assessed ethanol inhibition by the measuring ethanol-induced reduction of single-nAChR conductance.

At 400 mM ethanol, wild-type nAChR conductance was reduced by 16 ± 7.2% (*15*). Because the inhibition of wild-type by 400 mM EtOH is weak and the variability of the measurements is quite large, there is an approximately 3-fold bias in statistically analyzing these data toward mutations that increase, rather than decrease, ethanol sensitivity.[3] Therefore, a significance criterion (p) of ≤0.15 rather than ≤0.05 was chosen for mutations that reduced ethanol sensitivity.

The pattern of ethanol sensitivities in the set of α-M2 hydrophobic mutants (Figure 2) is very similar to that for hexanol. Three mutations (αL9′T, αS10′I, and αL11′S) caused highly significant changes ($p \leq 0.05$) in ethanol sensitivity. The αV13′S mutation reduced ethanol sensitivity ($p = 0.10$) in close parallel with its effect on hexanol sensitivity. The αT12′I mutation also reduced ethanol

[3] Because the reduction in wild-type nAChR conductance by 400 mM EtOH is so small (16 ± 7.2%), it is easier to demonstrate a significant sensitivity increase than a decrease in mutant receptors. If the same standard deviation is assumed for measurements in the mutants and wild type, a mutation must reduce the EtOH affinity 5-fold, but only enhance the EtOH affinity 2-fold to cause a significant change with p of ≤0.05. On the basis of the magnitude of the effects of αL8′S and αV13′S mutations, we infer that these side chains interact with EtOH bound to its pore site.

sensitivity, but not to a degree that reached statistical significance ($p = 0.83$). In addition, the αL8′S mutation, which had no effect on hexanol sensitivity, dramatically reduced ethanol sensitivity ($p = 0.12$). Ethanol inhibition, as assessed by channel conductance, appears to be affected by the same contiguous series of α-M2 amino acids that affect hexanol sensitivity (9′−13′) in addition to one additional amino acid (8′) closer to the inner end of M2.

DISCUSSION

An Inhibitory Patch Site. Our previous studies have demonstrated that hydrophobic mutations at αS10′ cause significant changes in the sensitivity of nAChR to inhibition by alcohol and volatile anesthetics. The data presented here extend the strategy of altering side chain hydrophobicity to 12 additional α-M2 domain positions, using two *n*-alcohols. We find that a small group of these mutations, located near the center of α-M2, significantly alter nAChR sensitivity to alcohols.

One crucial result of these studies is the identification of loss-of-sensitivity mutations in the α-M2 domain. Since the previously reported mutations at position 10′ increase hydrophobicity and increase sensitivity to alcohols (gain-of-sensitivity), it was possible that these position 10′ mutations created an alcohol-sensitive site where none previously existed (*10*). Since mutations that lower hydrophobicity at positions 8′, 9′, 11′, and 13′ reduce or obliterate *n*-alcohol inhibition, these residues very likely contribute to alcohol interactions with the wild-type nAChR site.

On the basis of our assumption that alcohol binding to the nAChR pore is primarily dependent on hydrophobic forces, we infer from our results that there is a common inhibitory site for ethanol and hexanol formed by four to five contiguous amino acids in the α-M2 domain. This finding suggests that alcohol inhibition is due to interactions with a large "patch" of the pore lining extending from an inner position of αL8′ to an outer position at αV13′. Alternatively, this region of the M2 domain, which has also been proposed to form the "gate" for ion permeation (*20*), may form an inhibitory unit that is influenced by both alcohols and hydrophobic mutations.

The αL8′S Mutation Differentially Affects Sensitivity to Ethanol and Hexanol. Hexanol and ethanol sensitivities are altered by mutations within a common region (αL9′−αV13′). However, the αL8′S mutation eliminates ethanol sensitivity while causing little change in hexanol sensitivity. This observation makes it far less likely that alcohols are allosterically influencing this region of the pore, since this model predicts that mutation effects are independent of the type of alcohol. It is therefore more likely that alcohols interact directly with this region of the pore lining, but at slightly different locations. One possibility is that ethanol, being smaller than hexanol and having a lower affinity for the site, is able to interact somewhat deeper in the pore. Conversely, the increased interaction surface between the outer pore lining and hexanol, reflected in its higher affinity, may prevent this larger alcohol from migrating further into the channel. Others have proposed that the homologous "ring" of leucines at position 9′ forms a narrowing of the pore (*20*), perhaps preventing hexanol interaction with the 8′ locus.

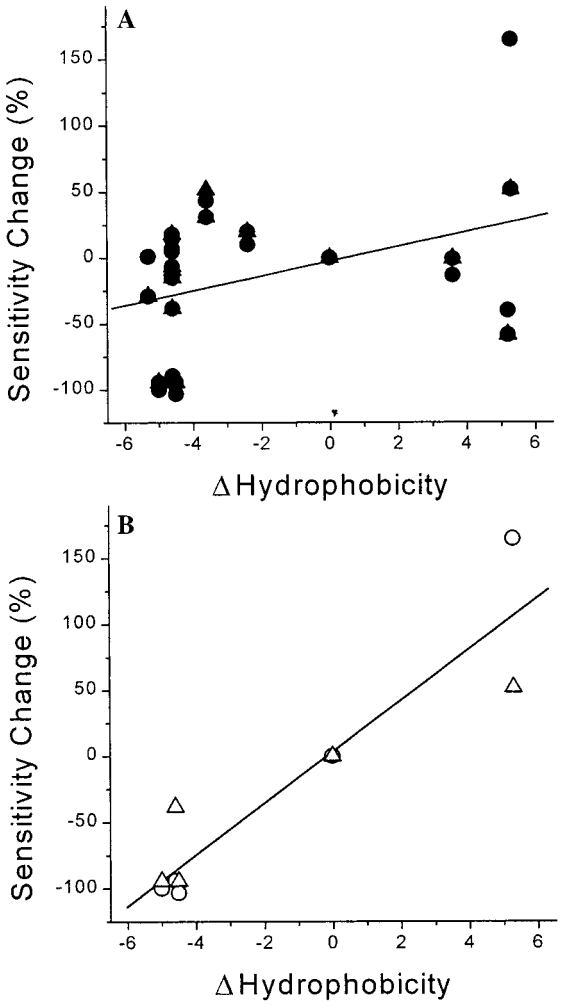

FIGURE 3: Strong correlation between side chain hydrophobicity and alcohol sensitivity localized to residues near the middle of α-M2. The percent sensitivity change from the wild-type value was calculated for the wild type and the 13 mutant nAChRs studied from the inhibition data in Figures 1 and 2 as $SC = 100\% \times (I_{mut} - I_{wt})/I_{wt}$. Each point represents the sensitivity change for either ethanol (circles) or hexanol (triangles) plotted against the side chain hydrophobicity change (Table 2). Correlations were determined from linear least-squares analysis. (A) There is no significant correlation between alcohol sensitivity and hydrophobicity for the entire data set ($R = 0.38$, $p = 0.10$). (B) Points for the four mutants that caused significant sensitivity changes to both hexanol and ethanol (αL9′T, αS10′I, αL11′S, and αV13′S) are depicted as open symbols, as is the wild-type value. There is a very strong correlation between alcohol sensitivity and hydrophobicity for these five receptors ($R = 0.93$, $p < 0.0001$).

The large size of the central inhibitory patch site and the differential impact of the αL8′S mutation on ethanol and hexanol sensitivity are important because they help explain why some pairs of compounds show mutually exclusive actions in the nAChR pore, while others do not. If it is assumed that the site extends significantly more than the 7.5 Å predicted in an α helix (discussed below), there is sufficient space to bind more than one molecule of ethanol (5−6 Å in length) or other short chain alcohols. Indeed, ethanol does not compete with long-chain alcohols for the inhibitory site on nAChR (*12*, *21*). Our mapping results suggest that ethanol occupies a position further toward the inner end of M2, allowing simultaneous binding of ethanol and a long-chain alcohol. Dilger and Vidal (*13*) studied the interaction of butanol and a charged blocker, QX-222,

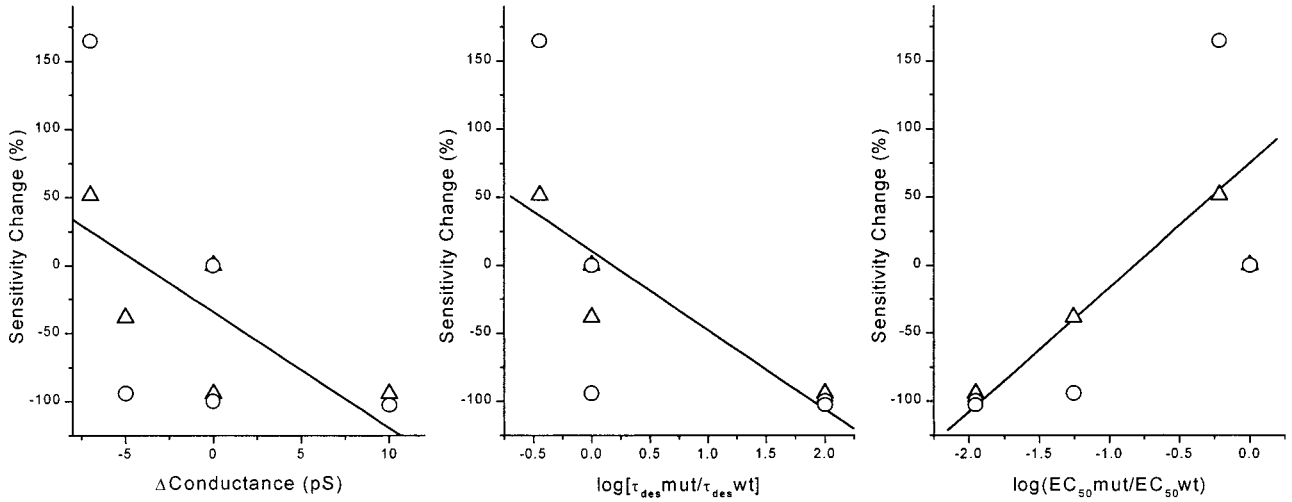

FIGURE 4: Correlations between alcohol sensitivity and conductance, desensitization, and gating in α-M2 hydrophobic mutants. For wild-type, αL9′T, αS10′I, αL11′S, and αV13′S nAChRs, changes in sensitivity to ethanol (○) and hexanol (△) were calculated as described in the legend of Figure 3 and plotted against the mutant-associated change in conductance, log(ratio of desensitization rates) or log(ratio of ACh EC_{50}s). Correlations were determined from linear least-squares analyses (—). Conductance: $R = -0.60$ and $p = 0.07$. Log τ_{des}: $R = -0.7$ and $p = 0.013$. Log EC_{50}: $R = 0.83$ and $p = 0.005$ (—).

concluding that both compounds could occupy the nAChR pore simultaneously. Mutagenesis and cysteine protection studies indicate that QX-222 interacts with residues αV13′, αS10′, and αS6′ (*22*, *23*). Thus, as suggested by Dilger, there is significant overlap between QX-222 and alcohol sites, but not enough to result in mutually exclusive occupation. In contrast to these examples, mutually exclusive inhibition of nAChR was observed with coapplication of *n*-heptanol and *n*-octanol (*7*). An additional factor is the differential interactions of various inhibitors with M2 domains from different nAChR subunits. Long chain alcohols apparently interact more intimately with α and β subunits than with γ or δ subunits (*11*), while QX-222 binding appears to be equally distributed among all subunits (*24*). Thus, the nAChR pore can accommodate only one molecule of heptanol or octanol (about 10 Å in length) at a time, but may be occupied simultaneously by two small alcohols or one small alcohol and a larger inhibitor.

Size versus Hydrophobicity in Mutants. At all the α-M2 loci where mutations caused significant sensitivity changes for both alcohols (9′−11′ and 13′), the changes in side chain hydrophobicity correlate strongly with changes in alcohol sensitivity (Figure 3, bottom). Altered sensitivity to ethanol also correlates with the hydrophobicity change for αL8′S. The strong correlation at the common inhibitory patch in the nAChR pore is consistent with the established correlation between nAChR blocker potency and hydrophobicity.

Of course, these mutations also alter side chain size (Table 2; *18*, *25*) so that, instead of hydrophobicity, steric factors might affect alcohol sensitivity. We have ruled out this alternative hypothesis in nAChRs using pairs of isosteric mutations at the α10′ locus (*15*), which demonstrate a very dominant effect of hydrophobicity over size. We have also investigated an isosteric pair of mutants at the 9′ locus. The αL9′V mutation causes no significant change in alcohol sensitivity, while the αL9′T mutant eliminates alcohol inhibition. Thus, side chain hydrophobicity is far more important than size in modulating the sensitivity of the nAChR inhibition site.

The sensitivity−hydrophobicity correlation is clearly not a general one for the entire set of α-M2 hydrophobic mutations (Figure 3, top), since the majority of mutations have little impact on alcohol sensitivity. A notable exception to the hydrophobicity correlation is the αT12′I mutation, which increases hydrophobicity, but decreases sensitivity to hexanol and modestly weakens ethanol inhibition. This mutation causes the largest decrease in conductance of all the mutants that have been studied (Table 2). We speculate that the αT12′I mutation may not be exposed directly to alcohols in the pore, but creates a local steric change, which reduces accessibility to the inhibitory patch site.

Do Other Functional Characteristics of nAChR Mutants Correlate with Anesthetic Sensitivity? For the subset of four α-M2 hydrophobic mutations that significantly affect sensitivity to ethanol and hexanol (αL9′T, αS10′I, αL11′S, and αV13′S), we find no significant correlation between alcohol sensitivity and channel conductance (Figure 4). However, there is a modest correlation between alcohol sensitivity and the maximal ACh-induced desensitization time constant and a strong correlation with EC_{50}. In this group of mutants, nAChRs with low EC_{50}s and slow desensitization are generally insensitive to alcohols, while those with higher EC_{50}s and fast desensitization are generally sensitive. EC_{50}s and desensitization in these mutants probably reflect the stability of their open-channel states (*26*, *27*), suggesting that perhaps alcohol inhibition is due not to channel block but to destabilization of the open state.

Arguing against this alternate hypothesis is evidence from several α-M2 mutants we studied that cause large changes in EC_{50} and/or desensitization rates, but have little impact on alcohol sensitivity. For example, the αT12′I and αL16′S mutants behave very much like both the αL9′T and αV13′S mutants, displaying low EC_{50}s and slow desensitization, but they do not exhibit extraordinary insensitivity to alcohol inhibition. The mutant with the highest EC_{50}, αL8′S, rather than displaying hypersensitivity to alcohols, is insensitive to ethanol and has normal sensitivity to hexanol. Other evidence against an open-state destabilization mechanism

comes from studies showing that ethanol stabilizes the nAChR open state, prolonging open channels and reducing the ACh EC_{50} (*19*, *28*), but it does not alter nAChR inhibition by long chain alcohols (*21*). Agonist binding, another determinant of EC_{50}, is also unlikely to influence alcohol sensitivity. Alcohols, unlike known competitive inhibitors of nAChRs, do not cause rightward shifts in ACh concentration−response studies. Also, mutations in the nAChR agonist binding domains that dramatically reduce ACh binding affinity, αY190F and αY198F (*29*), do not affect alcohol sensitivity (*19*).

Thus, agonist binding and open-channel stability are not mechanistically linked to alcohol inhibition, while correlations arise from a shared dependence on side chain hydrophobicity in the middle of the α-M2 domain. Additionally, structural determinants of gating and desensitization behavior in nAChRs are very broadly distributed, while determinants of hydrophobic blocker inhibition appear to be remarkably localized to the middle of the M2 domains. Of the mutant properties we have considered (Table 2), hydrophobicity is the only localized property that strongly influences alcohol sensitivity.

Implications for nAChR Pore Structure. While the methods used in this study cannot conclusively demonstrate interactions between alcohols and M2 domain residues, it seems reasonable to infer interactions between alcohols and those amino acid residues where mutations significantly alter sensitivity to inhibition, because complementary methods have demonstrated alcohol binding in this region of nAChRs as well as open-channel block by alcohols (see the introductory section). Since hexanol simultaneously interacts with all the nAChR subunits (*11*), it is also likely that alcohols occupy the central aqueous pore while contacting the inhibition site. By combining the concept of a central pore location with our current finding that most of the side chains near the middle of α-M2 may interact with alcohols, we can tentatively infer that the amino acid side chains from αL9′ through αV13′ (with the exception of αT12′) all face the aqueous pore. Thus, our data suggest that the midregion of α-M2 has a nonhelical structure in the open-channel state. This inference is in general agreement with other structural evidence. Unwin identified "bent rod" structures adjacent to the *Torpedo* nAChR pore and suggested that these were kinked M2 helices (*20*). Akabas et al. (*30*) have also suggested a nonhelical conformation in the middle of the α-M2 domain, based on a cysteine mutagenesis and chemical modification approach. In an α helix, the distance between αL8′ and αV13′ is predicted to be about 7.5 Å. If the secondary structure is nonhelical, this distance could be as large as 17 Å (e.g., β sheet structure).

Summary. Hydrophobic mutagenesis of nAChR α-M2 domain residues identifies a series of contiguous amino acids that influence inhibition by *n*-alcohols, extending from αL8′ or αL9′ to αV13′. Our data are most readily explained by the existence of a central inhibitory patch in the nAChR pore lining where interactions with alcohols are primarily due to hydrophobic forces. We further infer from our results that most of the residues in the central inhibitory patch are exposed to the aqueous environment of the pore when the channel is open. The large predicted length of the patch and the differential mapping of ethanol and hexanol interactions can account for why some pairs of nAChR inhibitors simultaneously occupy the pore, while other pairs of inhibitors exhibit mutually exclusive actions.

ACKNOWLEDGMENT

We thank Carol Gelb for her expert technical assistance. Dr. James McLaughlin (Medical University of South Carolina) and Michael M. White (Allegheny University) generously shared nAChR subunit clones.

REFERENCES

1. Franks, N. P., and Lieb, W. R. (1994) *Nature 367*, 607−614.
2. Diamond, I., and Gordon, A. S. (1997) *Physiol. Rev. 77*, 1−20.
3. Karlin, A., and Akabas, M. H. (1995) *Neuron 15*, 1231−1244.
4. McLarnon, J. G., Pennefather, P., and Quastel, D. M. J. (1988) in *Molecular and Cellular Mechanisms of Anesthetics* (Roth, S. H., and Miller, K. W., Eds.) pp 155−164, Plenum Publishing Corp., New York.
5. Lechleiter, J., and Gruener, R. (1984) *Proc. Natl. Acad. Sci. U.S.A. 81*, 2929−2933.
6. Dilger, J. P., and Brett, R. S. (1991) *Ann. N.Y. Acad. Sci. 625*, 616−627.
7. Wood, S. C., Tonner, P. H., de Armendi, A. J., Bugge, B., and Miller, K. W. (1995) *Mol. Pharmacol. 47*, 121−130.
8. Husain, S. S., Forman, S. A., Kloczewiak, M. A., Addona, G. H., Olsen, R. W., Pratt, M. B., Cohen, J. B., and Miller, K. W. (1999) *J. Med. Chem. 42*, 3300−3307.
9. Pratt, M. B., Husain, S. S., Miller, K. W., and Cohen, J. B. (2000) *Biophys. J. 78*, 360A (abstract).
10. Forman, S. A., Miller, K. W., and Yellen, G. (1995) *Mol. Pharmacol. 48*, 574−581.
11. Forman, S. A. (1997) *Biophys. J. 72*, 2170−2179.
12. Bradley, R. J., Sterz, R., and Peper, K. (1984) *Brain Res. 295*, 101−112.
13. Dilger, J. P., and Vidal, A. M. (1994) *Mol. Pharmacol. 46*, 169−175.
14. Dilger, J. P., Vidal, A. M., Mody, H. I., Boguslavsky, R., Lee, J., Katz, T., and Tall, E. (1996) *Prog. Anesth. Mech. 3*, 50−55 (abstract).
15. Forman, S. A., and Zhou, Q. (2000) *Alcohol.: Clin. Exp. Res.* (in press).
16. Forman, S. A. (1999) *Biochemistry 38*, 14559−14564.
17. Kyte, J., and Doolittle, R. F. (1982) *J. Mol. Biol. 157*, 105−132.
18. Chothia, C. (1976) *J. Mol. Biol. 105*, 1−14.
19. Forman, S. A., and Zhou, Q. (1999) *Mol. Pharmacol. 55*, 102−108.
20. Unwin, N. (1995) *Nature 373*, 37−43.
21. Wood, S. C., Forman, S. A., and Miller, K. W. (1991) *Mol. Pharmacol. 39*, 332−338.
22. Charnet, P., Labarca, C., Leonard, R. J., Vogelaar, N. J., Czyzyk, L., Gouin, A., Davidson, N., and Lester, H. A. (1990) *Neuron 4*, 87−95.
23. Pascual, J. M., and Karlin, A. (1998) *J. Gen. Physiol. 112*, 611−621.
24. Leonard, R. J., Labarca, C. G., Charnet, P., Davidson, N., and Lester, H. A. (1988) *Science 242*, 1578−1581.
25. Frommel, C. (1984) *J. Theor. Biol. 111*, 247−260.
26. Filatov, G. N., and White, M. M. (1995) *Mol. Pharmacol. 48*, 379−384.
27. Labarca, C., Nowak, M. W., Zhang, H., Tang, L., Deshpande, P., and Lester, H. A. (1995) *Nature 376*, 514−516.
28. Forman, S. A., Righi, D. L., and Miller, K. W. (1989) *Biochim. Biophys. Acta 987*, 95−103.
29. Tomaselli, G. F., McLaughlin, J. T., Jurman, M. E., Hawrot, E., and Yellen, G. (1991) *Biophys. J. 60*, 721−727.
30. Akabas, M. H., Kaufmann, C., Archdeacon, P., and Karlin, A. (1994) *Neuron 13*, 919−927.
31. Miller, C. (1989) *Neuron 2*, 1195−1205.

BI001281Q